

A GENERAL AVIATION AIRCRAFT CONCEPTUAL DESIGN USING MULTIDISCIPLINARY OPTIMIZATION

Keen I. Chan^{} & Antoine A. Vincent[†]*

Gas Turbine Laboratory
Massachusetts Institute of Technology

ABSTRACT

The characteristics and performances of a general aviation aircraft are optimized using a multidisciplinary numerical model of the airplane, and the iSIGHT optimizer. The model consists of aerodynamics, structures, weight, range and propulsion modules. It takes as inputs the aircraft geometry and flight conditions, and outputs a range to be maximized and a gross takeoff weight to be minimized.

The algorithm was validated by the *Cessna 172R Skyhawk* example, also used as a starting point for the gradient-based optimizations. A single-objective Sequential Quadratic Programming (SQP) optimization targeting range alone allows a 81% increase in range, at the expense of a 65% rise in weight. A multi-objective SQP optimization allows keeping the increase in range while limiting the rise in weight to 53%. An appropriate scaling reduces the number of iterations by a threefold factor.

The constraints on fuselage ratio, wing bending stress and wing aspect ratio severely limit the feasible range of the design space. As a result, most designs explored by a genetic algorithm were infeasible, so that this heuristic technique does not yield any further improvement.

This study could be easily extended by refining the range module. Moreover, a better exploration of the feasible design space would be decisive to improve the results.

1 -INTRODUCTION

With the increasing available computation power, Multidisciplinary System Design Optimization (MSDO) has been extensively implemented in the preliminary design phase to perform optimization of numerical models consisting of several different modules. As they include structures, aerodynamics, propulsion and performance issues, aircrafts are ideally suited for this kind of study.

Our goal is to optimize the range and the gross take-off weight of a general aviation aircraft. More precisely, we are focused on a single engine piston aircraft, taking as a basic example the *Cessna 172R Skyhawk* familiar to most flight simulator users. This leads us to put reasonable constraints on the aircraft geometry and performances.

First, we draw the outline of the simulation numerical modules, and see how they are validated. Then we discuss the results of the single objective SQP range optimization, and we stress the importance of an appropriate scaling, as well as the role of the constraints.

Afterwards, we set up a multi-island genetic algorithm to explore new regions of the design space. This study is followed by a multi-objective approach, and a determination of the Pareto front. We finish with a summary of the previous elements, and with a few suggestions for further work.

2 - NOMENCLATURE

D	Drag force (N)
D_F	Fuselage diameter (m)
D_B	Blade diameter (m)
\vec{g}	Inequality constraint vector
h	Cruise altitude (m)
\vec{J}	Objective vector
L	Lift force (N)
L_F	Fuselage length (m)
L_W	Wing span (m^2)
M_E	Engine weight (kg)
M_F	Fuel weight (kg)
M_P	Payload weight (kg)
M_{TO}	Gross takeoff weight (kg)
N_E	Number of engines
N_P	Number of passengers
\vec{p}	Fixed parameters vector
P_E	Engine power (W)
R	Range (km)
r_F	Fuselage ratio
r_W	Wing aspect ratio
sfc	Specific fuel consumption (m^{-1})
S_W	Wing area (m)
V	Cruise velocity (m)
\vec{x}	Design variable vector
α_P	Fraction of power at cruise
λ_R	Objective weight for the range
λ_W	Objective weight for the gross takeoff weight
η_P	Propulsive efficiency
ρ	Air density at cruise
σ	Wing bending stress (MPa)
ω	Propeller rotation velocity (rpm)

Subscript

0 *Cessna 172R Skyhawk* value

Superscript

* Single-objective SQP optimum value

3-PROBLEM FORMULATION

3.1 Mathematical definition

The design of a general aviation aircraft is optimized initially for maximum range R and subsequently with the additional objective of minimum M_{TO} . For that purpose, we modify the variables in the design vector $x=[S_W, L_W, L_F, D_F, V, h]^T$: the wing area, the wing span, the fuselage length, the fuselage diameter, the cruise velocity and the cruise altitude. More formally, this can be written as:

$$\max \vec{J}(\vec{x}, \vec{p}) = \max \begin{bmatrix} R(\vec{x}, \vec{p}) \\ -M_{TO}(\vec{x}, \vec{p}) \end{bmatrix}$$

subject to:

$$\vec{g}(\vec{x}, \vec{p}) = \begin{bmatrix} \sigma - 2000 \\ 5 - r_W \\ 1 - r_F \end{bmatrix} \leq 0$$

$$0 \leq S_W$$

$$0 \leq L_W \leq 20$$

$$3 \leq L_F \leq 20$$

$$1 \leq D_F \leq 4$$

$$0 \leq V$$

$$0 \leq h \leq 6000$$

3.2 - Bounds of design space

The bounds of the design vector were set as follows. As we cannot consider negative area or length, we had to set lower limits to zero. An aircraft whose fuselage length is lower than 3 meters seems improbable. Wing span and fuselage length are assumed to be less than 20 meters to allow the aircraft to fit easily in a standard hangar. A fuselage diameter constrained between 1 and 4 meters seems reasonable for an aircraft of this category. Finally, 6000 meters is the ceiling for Visual Flight Rules. As can be seen in Table 1, these values are compatible with the Cessna case.

Design variable	Min	x_0	Max
S_W	0	16.2	-
L_W	0	11	20
L_F	3	8.28	20
D_F	1	1.22	4
V	0	62.78	-
h	0	2438	6000

Table 1 – Design variable boundaries

3-3 Other constraints

The upper limit constraint on the wing bending stress $\sigma < 2000 MPa$ set previously corresponds to the yield strength of carbon fiber material. The fuselage ratio is defined as:

$$r_F = \frac{D_F}{L_F} \geq 0.1$$

The lower limit allows the proportions of the aircraft to remain reasonable: without it, optimum aircraft would often look like a flying cigar.

In the same way, the wing aspect ratio is defined as:

$$r_W = \frac{(L_W)^2}{S_W} \geq 5$$

This lower limit allows the final aircraft to differ from a flying wing full of fuel when optimization is carried out.

3.4 Fixed parameters

The fixed parameters and their corresponding values are shown in Table 2 below.

Parameter	Value	Parameter	Value
P_E	160 bhp	D_E	1.91 m
M_E	70 kg	N_E	1
$sf\hat{c}$	$5 \cdot 10^{-6} \text{ m}^{-1}$	M_P	100
α_p	80%	N_P	2
ω	2400 rpm		

Table 2 - Values of fixed parameters

4 SIMULATION MODEL

4.1 Model outline

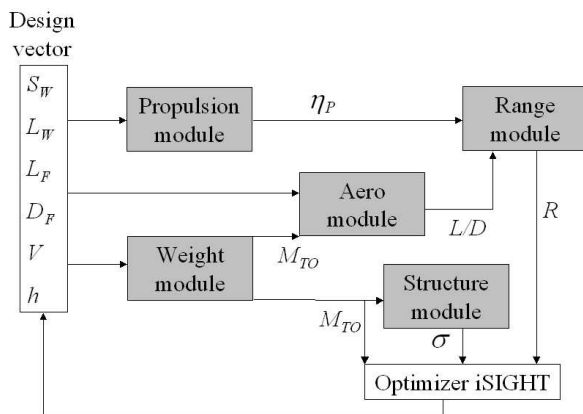


Figure 1 – Simulation model

The simulation model illustrated in Figure 1 is composed of five different parts: a propulsion module, a range module, an aerodynamics module, a weight module and a structures module. The simulation code itself is a C program, and uses ASCII files to communicate with the optimizer functions of iSIGHT.

The simulation code structure is relatively straightforward, because it does not include any feedback loop, as illustrated by the N² diagram in Figure 2.

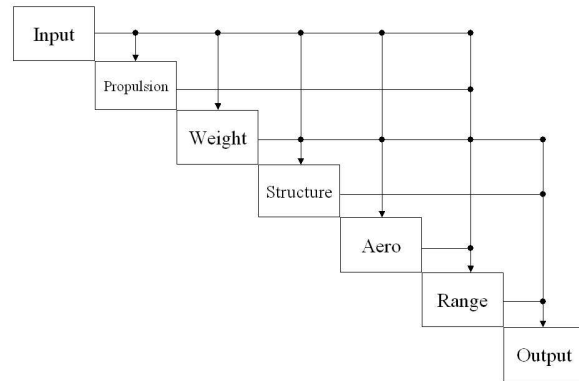


Figure 2 – N² diagram

Knowing the cruise altitude that is part of the design vector, an ICAO standard atmosphere table allows us to compute by linear interpolation the corresponding air viscosity and air density.

4.2 Weight module

The gross takeoff weight is assumed to be the sum of the empty weight, the fuel weight, the payload weight and the passenger weight. As we saw it, the payload weight and passenger numbers are fixed parameters. Assuming that fuel is stored in the wing, the fuel weight is estimated from the wing surface and the wing span. Finally, the empty weight is computed from an estimate of each of the components of the aircraft.

4.3 Structures module

In order to compute the wing bending stress, we assume that the wing is subject to the moment due the lift force, and to the moment due to the wing weight. If we consider the wing spar as a hollow tube of constant circular cross-section with a fixed thickness, we can derive its second inertia moment:

$$I = \frac{\pi(r_0^4 - r_i^4)}{4}$$

The wing bending stress is then determined using:

$$\sigma = \frac{M_{TO} k_0}{2I}$$

As seen above, it is important that the wing bending stress remains below the material yield strength.

4.4 Aerodynamics module

The aerodynamics module computes the lift to drag ratio used by the range module. As we consider a stationary flight at cruise, we can assume that the lift is equal to the aircraft weight.

A great deal of attention is paid to obtain a proper estimate of the drag, which is decomposed in wing drag, tail drag, fuselage drag and interference drag.

4.5 Propulsion module

The implementation of this module starts by computing the power coefficient K_p and the advanced ratio K_a defined respectively as:

$$K_p = \frac{P_E}{\rho \omega^3 D_B^5}$$

$$K_a = \frac{V}{\omega D_B}$$

A bilinear interpolation from a digitized efficiency graph for a 3 bladed propeller aircraft yields then the propulsive efficiency:

$$\eta_p = f(K_p, K_a)$$

4.6 Range module

The range module takes its input from the weight, aerodynamics and propulsion module, and is implemented as a classical Breguet range equation:

$$R = \eta_p \frac{L}{D} \frac{V}{g \cdot sfc} \log \left(\frac{M_{TO}}{M_{TO} - 0.85 \cdot M_F} \right)$$

4.7 Algorithm validation

The modules are tested by inputting the reference values as listed in Tables 1 and 2, and comparing the resulting R and M_{TO} with those of the actual Cessna 172R. The nominal Cessna values are $R = 1074$ km and $M_{TO} = 1111$ kg. The values obtained from our algorithm are $R = 1218$ km (+13%) and $M_{TO} = 1309$ kg (+18%). The reasonable agreement obtained indicates that further work on optimizing the initial design can be proceeded with.

5 - DESIGN SPACE EXPLORATION

A parameter study is performed about the design point as shown in Table 1, which are actually those of the Cessna 172R Skyhawk. Each of the design variables is allowed to vary about the design point and the variation of range is observed. The results of the parameter study are plotted in Figs. 3 to 8. The shaded region in each of Figs. 3, 4, 6 and 7 indicates an infeasible region in which at least one constraint is violated.

■ Cessna 172R Skyhawk

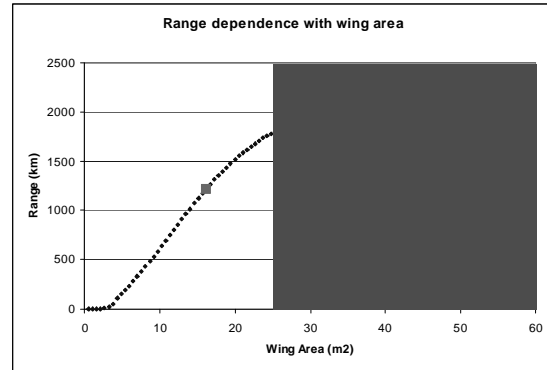


Figure 3 - Variation of Range with Wing Area

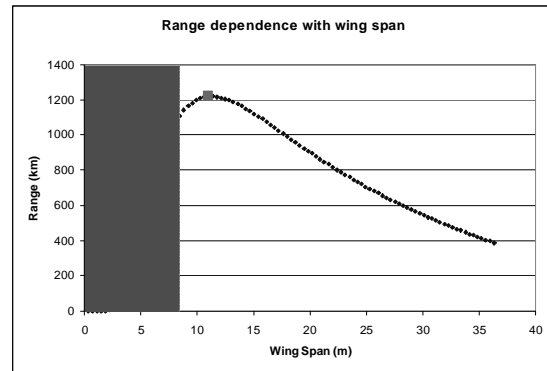


Figure 4 - Variation of Range with Wing Span

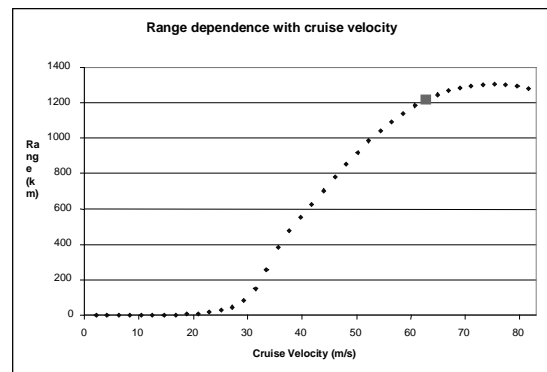


Figure 5 - Variation of Range with Cruise Velocity

6 SINGLE-OBJECTIVE OPTIMIZATION

6.1 Gradient Search Results

The design is optimized for maximum R using the optimization program iSIGHT. A gradient search technique, Sequential Quadratic Programming (SQP), is selected. This creates a quadratic approximation to the Lagrangian function and linear approximations to the constraints. The quadratic problem is solved to obtain the search direction. An update to the Lagrangian is made upon reaching a new design point along the search direction. This technique is widely used in engineering applications and is presently considered to be the best gradient-based algorithm with strong theoretical basis. However, it does not assure the location of a global optimum.

Using SQP, the results obtained are shown in Table 3.

Variables	Lower bound	Initial point x_0	Optimum x^*	Upper bound
S_W	0	16.2	35.0	-
L_W	0	11	13.2	20
L_F	3	8.28	5.74	20
D_F	1	1.22	1.0	4
V	0	62.78	58.4	-
h	0	2438	2448	6000
R		1218	1940	
M_{TO}		1309	1829	
σ			2000	2000
r_W	5	7.47	5.0	
r_F	0.1	0.147	0.174	

Table 3 - SQP Optimization results

It can be seen that the range obtained by SQP is an improvement over that of the Cessna 172R. The constraints on D_F , σ and r_w have become active.

6.2 Sensitivity Analysis

The definition of normalized sensitivity of R with respect to a design variable x_i about an optimum design vector \mathbf{x}^o is

$$\text{Normalized Sensitivity } y = \frac{x_{i,o}}{R(\mathbf{x}_o)} \cdot \frac{\partial R}{\partial x_i} \Big|_{\mathbf{x}_o}$$

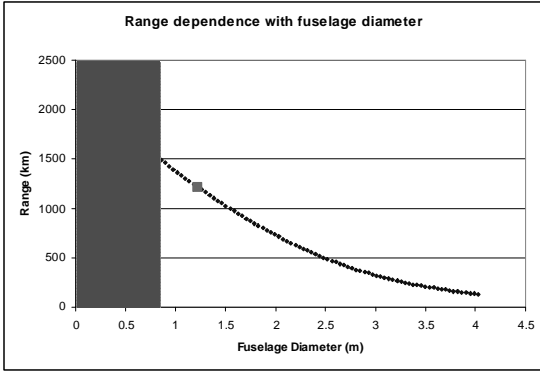


Figure 6 -Variation of Range with Fuselage Diameter

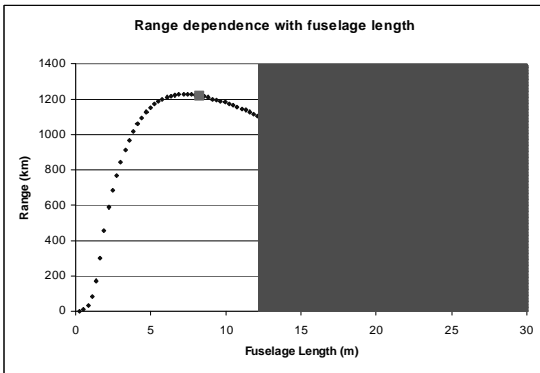


Figure 7 - Variation of Range with Fuselage Length

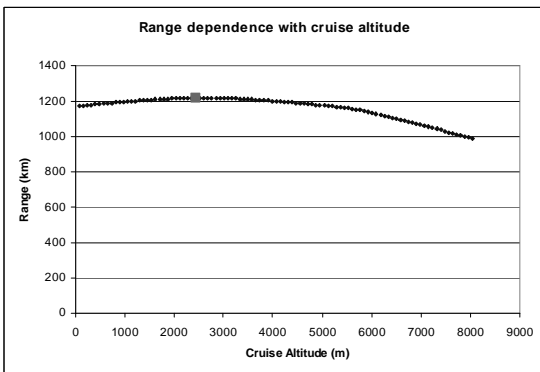


Figure 8 - Variation of Range with Cruise Altitude

The results indicate that to increase range towards a maximum, wing area should be increased and fuselage diameter reduced (Figs. 3 and 6). The other plots of Figs. 4, 5, 7 and 8 indicate their respective design variables as already being close to optimal.

This is calculated for each of the design variables, with finite differencing being used to calculate the derivative term. The sensitivities with respect to each variable are shown in Figure 9.

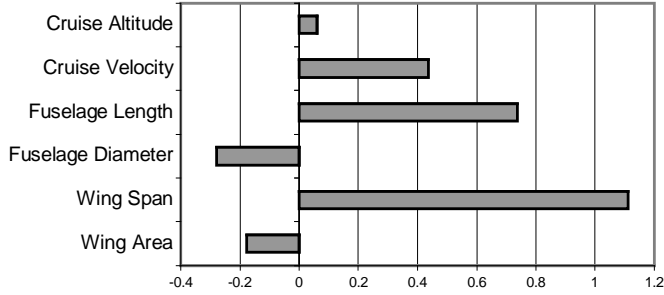


Figure 9 – Normalized sensitivity at SQP optimum

It can be seen that at the present optimum, range is most sensitive to wing span S_w and fuselage length L_F .

6.3 Relaxation of constraints

Initializing the SQP algorithm from the Cessna design \mathbf{x}_0 , we relax successively the three constraints that were active at \mathbf{x}^* , and report the results of the optimization in Table 4.

Variables	x_{\min}	x^*	$\sigma + 25\%$	$D_F + 25\%$	$r_F + 25\%$	x_{\max}
S_W	0	35.0	62.22	35.05	106.5	-
L_W	0	13.2	17.64	13.25	20	20
L_F	3	5.74	10	6.45	14.34	20
D_F	1	1.0	1.0	0.75	1.43	4
V	0	58.4	64.97	58.4	73.3	-
h	0	2448	4693	2448	2450	6000
R		1940	3664	2258	3905	
M_{TO}		1829	3384	1777	6925	
σ		2000	2500	2000	2000	2000
r_W	5	5.0	5.0	5.0	3.75	
r_F	0.1	0.174	0.1	0.116	0.1	

Table 4 – Effects of relaxation of constraints

When we relax the wing bending stress constraint by 25%, we observe that the range increases by 89%, but

so does also the gross takeoff weight. In comparison, if we relax by 25% the constraint on the fuselage diameter, the range is only increased by 16%. The main constraint at \mathbf{x}^* appears to be the fuselage ratio constraint: if we relax it by 25%, the range increases by 101%. Simultaneously, the gross takeoff weight increases by 279%, which constitutes clearly a too high price to pay.

6.4 Single objective scaling

In order to improve the optimization process, it is important to determine an appropriate scaling. As beforehand, we regard the range as the only objective, provided that the constraints are satisfied. To compute the diagonal coefficients of the Hessian matrix of the objective, standard finite difference formulations are employed:

$$\frac{\partial^2 R}{\partial x_i^2}(\mathbf{x}^*) = \frac{R(x_i + \delta x_i) - 2R(x_i) + R(x_i - \delta x_i)}{\delta x_i^2}$$

From the diagonal coefficients of the Hessian at the SQP optimum, we can set up appropriate scaling factors, and we check their relevance by computing the new Hessian diagonal coefficients taking scaling into account. The results are summarized in Table 5.

Design variable	Original Hessian coefficient	Scaling Factor	New Hessian coefficient
S_W	-3.05	1	-3.05
L_W	-38.59	10	-0.386
L_F	-79.28	10	-0.773
D_F	-139.1	10	-1.378
V	-1.564	1	-1.564
h	0.0136	0.1	0.0045

Table 5 – Scaling and Hessian coefficients

Except for the altitude, the scaling factors are appropriate, as the new Hessian coefficients are of the order of magnitude of one. The failure for the altitude may be explained by the computation step δx_i , which may not be appropriate in that case.

Starting from the Cessna design with these scaling factors, we obtain the same SQP optimum, but the number of iterations necessary to achieve convergence is reduced by a threefold factor from 157 to 54.

7 SINGLE-OBJECTIVE HEURISTIC OPTIMIZATION

Population	x*	5 islands of 5	10 islands of 5	10 islands of 10	5 islands of 5	5 islands of 5
Mutation rate	-	0.01	0.01	0.01	0.001	0.1
S_W	35.0	21.03	63.39	73.68	58.22	19.61
L_W	13.2	10.33	15.97	16.93	16.48	10.10
L_F	5.74	3.63	14.00	17.22	4.42	3.84
D_F	1.0	2.73	1.05	1.02	1.37	3.98
V	58.4	49.10	67.49	78.78	57.38	22.61
h	2448	2579.5	5132.50	101.02	1089.8	5331.
R	1940	254.13	3821.96	5426.7	1326.0	3.68
σ	2000	1952	1862	1959	1883	1741.
r_W	5.0	5.08	4.02	3.89	4.67	5.20
r_F	0.174	0.76	0.075	0.059	0.31	1.04

Table 6 – Genetic Algorithm results

We use the standard iSIGHT multi-island genetic algorithm to perform a heuristic optimization. The goal of this study is to explore different regions of the design space from the ones studied by the gradient-based method. By running the algorithm for 40 generations, we obtain a reasonably constrained computation time that does not exceed an hour. We try diverse population sizes and mutation rates, as described in Table 6. In this table, figures indicating an infeasible design due to a constraint violation appear in bold fonts.

Compared to the SQP optimum, the first run with 5 islands of 5 persons is quite disappointing, as the range is only 254 km. Keeping the same mutation rate of 0.01%, if we try to increase the population size by rising the number of islands or inhabitants per islands, we obtain infeasible designs, although the overall range is actually increased. If we reduce the mutation rate by a tenfold factor, the range falls to 1326 km. And if we increase the mutation rate by a tenfold factor, we obtain a small range of 3.68 km.

As a conclusion, the single-objective genetic algorithm was not able to improve the SQP optimum design. This can be explained by the importance of constraints that make most of the design explored by the genetic algorithm infeasible.

8 BI-OBJECTIVE OPTIMIZATION

8.1 Bi-objective results

From now onwards, we try to maximize the range and simultaneously to reduce the gross takeoff weight. As both objectives are of the same order of magnitude, in the range of a few thousands, objective scaling factors are not necessary. We perform iSIGHT weighted sum approach with the Sequential Quadratic Optimization algorithm, where the overall objective is a linear combination of range and gross takeoff weight:

$$J = \lambda_R \cdot R - \lambda_W \cdot W$$

The range maximization and gross takeoff weight minimization are clearly conflicting objectives. Indeed, an increase in range can easily be carried out by an increase in fuel weight, which in return increases the overall weight of the aircraft. Results for different values of the weight factors are presented in Table 7.

The case 2 shows that with a proper choice of scaling coefficients, it is possible to keep the range obtained using the single-objective SQP algorithm, and to reduce the gross take-off weight by 7.9%. As a result, we can reasonably say that the multi-objective approach is successful. The case 3 shows what happens when we put more emphasis on the gross takeoff weight than on the range, as it is usually done in classical aeronautics preliminary design practice. We obtain an aircraft of 1156kg and with a range of 1265km: its geometric configuration and its performances are relatively close to the Cessna case x_0 .

Variables	x_0	x*	Case 1	Case 2	Case 3
λ_R	-	1	2	2.50	1
λ_W	-	0	1	1	2
S_W	16.2	35.04	30.74	31.50	18.5
L_W	11	13.24	12.39	12.55	9.62
L_F	8.28	5.75	5.83	5.742	4.758
D_F	1.22	1.0	1.0	1.0	1.0
V	62.78	58.37	61.24	62.36	63.03
h	2438	2445	2447	2998	2447
R	1074	1940	1893	1937	1265
M_{TO}	1111	1830	1655	1686	1156
σ		2000	2000	2000	2000
r_W	7.47	5	5	5	5
r_F	0.147	0.174	0.172	0.174	0.21

Table 7 – Bi-objective optimization results

8.2 Pareto front

An easy way to visualize the range-weight tradeoff is to determine the Pareto front. The full-factorial approach was attempted, but it was decided to restrict the study range to a narrow region around the SQP single-objective optimum, as specified in Table 8.

Design variable	Min	Max	Number of levels
S_W	30	40	5
L_W	10	20	5
L_F	10	13	6
D_F	0.8	4	8
V	50	70	4
h	2000	3000	4

Table 8 Parameters for full-factorial exploration

According to this table, we explore 19200 design configurations. If we try to increase the number of explored levels, the computation time reaches several hours. And if we attempt to enlarge the range of the explored region of the design space, the number of feasible designs drops significantly. Using the current configuration, 2544 runs are feasible.

It is obvious that the Pareto front represented on Figure 10 is not accurate, as we do not explore the whole design space. However, it clearly exhibits the tradeoff between a low gross takeoff weight and a high range.

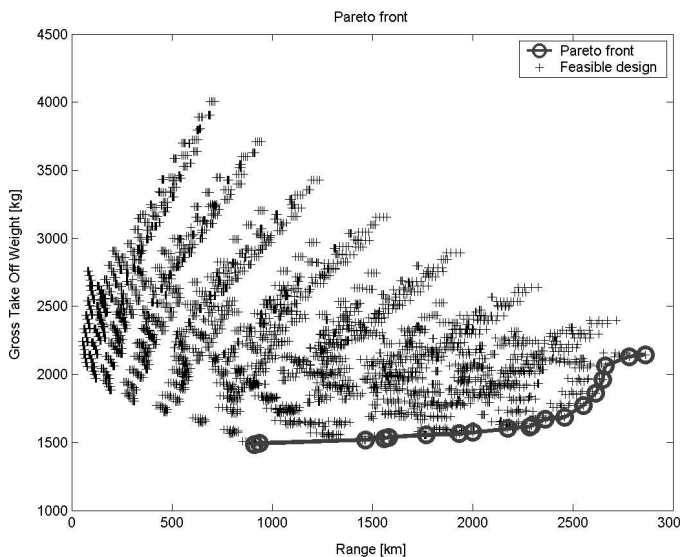


Figure 10 - Pareto front

9 CONCLUSIONS

Through a single objective SQP optimization, we were able to increase the range by 59%, at the expense of a concurrent increase in gross take-off weight. Starting from the same initial design vector, the choice of appropriate scaling factors accelerated the algorithm convergence speed by a threefold factor. At the optimum, the normalized sensitivity of the range is greatest with respect to the wing span and the fuselage length.

At the SQP optimum, three constraints are active, and by releasing independently each of them, we can achieve a significant improvement in range, while the aircraft becomes physically meaningless. Actually, most of the design space prescribed by the lower and upper bounds is made of infeasible designs. This explains the failure of the heuristic approach through a multi-island genetic algorithm, as most of the explored designs were infeasible.

When we carry out a multi-objective weighted sum approach incorporating the minimization of the gross takeoff weight, we can keep the range obtained previously, and decrease concurrently the aircraft weight by 7.9%. When we increase the weight of the gross take off weight in the cumulative objective function, this yields aircraft characteristics and performances very similar to the reference Cessna: this reflects well the industrial practice to put the emphasis on weight minimization.

Future work ideally aims at improving the accuracy of the model, which currently predicts performances of the Cessna within a 20% error margin. A better estimate of the aircraft gross take off weight seems especially critical. Moreover, the constraints on the fuselage and wing aspect ratio appear *per se* relatively arbitrary, as they are set at the optimizer level. They probably indicate that our simplistic model does not take into account some critical physical phenomenon.

A deeper knowledge of which part of the design space is actually feasible would also be particularly valuable. As there are three constraints and eight design variables, this would require an extensive study. However, this step may allow us to set up properly the genetic algorithm in order to explore different parts of the design space.